

HOLOGRAPHICS

Combining Holograms with Interactive Computer Graphics

Oliver Bimber
Bauhaus-University Weimar, Media Faculty, Dept. Augmented Reality
Bauhausstr. 11, 99423 Weimar, Germany
Tel.: +49-(0)3643-583724, Fax: +49-(0)3643-583709, Email: obimber@computer.org

TABLE OF CONTENT

1 Introduction

2 Digital Light For Reconstructing Holograms

- 2.1 Partially Reconstructing Object Waves
- 2.2 Modifying Amplitude Information

3 Extracting Depth Information from Holograms

- 3.1 Depth Reconstruction Using Flatbed Scanners
- 3.2 Depth Reconstruction Using Range Scanners

4 Interacting With Augmented Holograms

- 4.1 Display Prototypes
- 4.2 Increasing Viewing Range With Multiplex Stereograms
- 4.3 Holographic Windows
- 4.4 Force-Feedback Interaction
- 4.5 Touch Interaction
- 4.6 Augmenting Volumetric Multiplexed Holograms

5 Augmenting Large-Scale Holograms

- 5.1 Using The Grating As Diffuser
- 5.2 Using Shuttered Projection Screens

6 Conclusion

1. INTRODUCTION

Among all imaging techniques that have been invented throughout the last decades, computer graphics is one of the most successful tools today. Many areas in science, entertainment, education, and engineering would be unimaginable without the aid of 2D or 3D computer graphics. The reason for this success story might be its interactivity, which is an important property that is still not provided efficiently by competing technologies – such as holography.

While optical holography and digital holography are limited to presenting a non-interactive content, electroholography or computer generated holograms (CGH) facilitate the computer-based generation and display of holograms at interactive rates [2,3,29,30]. Holographic fringes can be computed by either rendering multiple perspective images, then combining them into a stereogram [4], or simulating the optical interference and calculating the interference pattern [5]. Once computed, such a system dynamically visualizes the fringes with a holographic display. Since creating an electrohologram requires processing, transmitting, and storing a massive amount of data, today's computer technology still sets the limits for electroholography. To overcome some of these performance issues, advanced reduction and compression methods have been developed that create truly interactive electroholograms. Unfortunately, most of these holograms are relatively small, low resolution, and cover only a small color spectrum. However, recent advances in consumer graphics hardware may reveal potential acceleration possibilities that can overcome these limitations [6].

In parallel to the development of computer graphics and despite their non-interactivity, optical and digital holography have created new fields, including interferometry, copy protection, data storage, holographic optical elements, and display holograms. Especially display holography has conquered several application domains. Museum exhibits often use optical holograms because they can present 3D objects with almost no loss in visual quality. In contrast to most stereoscopic or autostereoscopic graphics displays, holographic images can provide all depth cues—perspective, binocular disparity, motion parallax, convergence, and accommodation—and theoretically can be viewed simultaneously from an unlimited number of positions. Displaying artifacts virtually removes the need to build physical replicas of the original objects. In addition, optical holograms can be used to make engineering, medical, dental, archaeological, and other recordings—for teaching, training, experimentation and documentation. Archaeologists, for example, use optical holograms to archive and investigate ancient artifacts [7,8]. Scientists can use hologram copies to perform their research without having access to the original artifacts or settling for inaccurate replicas.

Optical holograms can store a massive amount of information on a thin holographic emulsion. This technology can record and reconstruct a 3D scene with almost no loss in quality. Natural color holographic silver halide emulsion with grain sizes of $8nm$ is today's state-of-the-art [14].

Today, computer graphics and raster displays offer a megapixel resolution and the interactive rendering of megabytes of data. Optical holograms, however, provide a terapixel resolution and are able to present an information content in the range of terabytes in real-time. Both are dimensions that will not be reached by computer graphics and conventional displays within the next years – even if Moore's law proves to hold in future.

Obviously, one has to make a decision between interactivity and quality when choosing a display technology for a particular application. While some applications require high visual realism and real-time presentation (that cannot be provided by computer graphics), others depend on user interaction (which is not possible with optical and digital holograms). Consequently, holography and computer graphics are being used as tools to solve individual research, engineering, and

presentation problems within several domains. Up until today, however, these tools have been applied separately. The intention of the project which is summarized in this chapter is to combine both technologies to create a powerful tool for science, industry and education. This has been referred to as *HoloGraphics*. Several possibilities have been investigated that allow merging computer generated graphics and holograms [1]. The goal is to combine the advantages of conventional holograms (i.e. extremely high visual quality and realism, support for all depth queues and for multiple observers at no computational cost, space efficiency, etc.) with the advantages of today's computer graphics capabilities (i.e. interactivity, real-time rendering, simulation and animation, stereoscopic and autostereoscopic presentation, etc.). The results of these investigations are presented in this chapter.

The remainder of this chapter is organized as follows: Section 2 summarizes the general concept of digitizing the reconstruction wave that replay a hologram. It also describes real-time rendering algorithms for achieving these effects. Spatial distribution, amplitude and wavelength can be controlled to augment holograms consistently with graphical elements. Since depth information of both –holographic and graphical content– is essential for the described approaches, section 3 presents results of using flat bed scanners and range scanners for estimating holographic depth information. Section 4 discusses several interaction forms in combination with different hologram types and describes current experimental display configurations. It is shown how the viewing range of augmented holograms can be increased with the aid of multiplex stereograms and how augmented holograms can be embedded into windows-oriented desktop workplaces. Furthermore, it is demonstrated how force-feedback and touch-interaction can be applied to augmented holograms, and how to combine volumetric multiplexed holograms with stereoscopic graphics. Section 5 discusses possibilities of augmenting large scale holograms using shuttered projection screens. It compares this active technology with the application of passive holographic projection screens and with a direct projection onto the holographic grating without additional diffuser. Finally, section 6 concludes this chapter and discusses future potentials.

2. DIGITAL LIGHT FOR RECONSTRUCTING HOLOGRAMS

The two basic hologram types—transmission and reflection—are both reconstructed by illuminating them with spatially coherent light (i.e. using a point-source of light). These two types have generated a number of variations. Although some holograms can be reconstructed only with laser light, others can be viewed under white light.

Conventional video projectors represent point sources that are well suited for viewing white-light reflection or transmission holograms. Early experiments with video projectors for reconstructing optical holograms have been made in the art and engineering domains. In some art installations, optical holograms have been linked with time-based media, such as slides, film-loops or color effects that are projected onto them to achieve artistic effects [15,16]. Others have redirected projected light with multiple mirrors to simulate multiple different light sources. The goal was to achieve dynamic fluctuation effects with optical holograms [17,18].

Today's high-intensity discharge lamps of projectors can produce a very bright light. The main advantage for using video projectors instead of analog light bulbs is that the reference wave used to reconstruct the hologram can be digitized. Thus it is possible to control the amplitude and wavelength of each discrete portion of the wavefront over time [1]. Today's computer graphics

capabilities allow merging any kind of two-dimensional or three-dimensional graphical elements seamlessly with the recorded holographic content – potentially leading to efficient visualization tools that combine the advantages of holography and computer graphics.

A hybrid display approach has already been described earlier that combined a transmission hologram with a liquid crystal display to realize a new user interface for business machines, such as photocopiers [19]. In this case, a normal light bulb was used to illuminate a transmission hologram which was mounted behind an LCD panel. Since the light source was analog, it was not possible to control the reconstruction of the holographic content. Electronically activated two-dimensional icons that were displayed on the LCD appeared simultaneously and unregistered with the three-dimensional hologram. As mentioned above, video projectors allow digitizing the reference wave, which leads to a seamless integration of graphical elements into an optical hologram.

Figure 1 shows the projected reference wave (top row) in different states, and the resulting holographic image (bottom row) of a monochrome white-light reflection hologram. A uniform reference wave reconstructs the entire hologram uniformly (first column of fig. 1). Selectively emitting light in different directions allows creating an incomplete reference wave that reconstructs the hologram only partially (second column of fig. 1). Local amplitude variations in the reference wave result in proportional amplitude variations in the reconstructed object wave (third column of fig. 1). Variations in wavelength do not lead to useful effects in most cases due to the wavelength dependency of holograms (fourth column of fig. 1). But this is still a matter for further investigations. One example for encoding color information into the reference wave is described in section 4.6.

Reconstructing the object wave only partially using a digital reference wave is the key concept of integrating graphical elements into an optical hologram. Technically, optical combiners such as mirror beam combiners or semi-transparent screens can be used to visually overlay the graphical output rendered on a screen over a holographic plate. In this case, however, the reconstructed light of the hologram will interfere with the overlaid light of the rendered graphics and an effective combination is impossible (cf. figure 19d, for example). However, the holographic emulsion can be used as optical combiner itself, since it is transparent if not illuminated in the correct way. Raster displays can be placed behind the holographic film and projected light can be used for replaying the hologram in a controlled way – synchronized with the presentation of the graphical components.

If autostereoscopic displays, such as parallax displays are used to render 3D graphics registered to the hologram, then both holographic and graphical content appear three-dimensional within the same space. This is also the case if stereoscopic displays with special glasses that separate the stereo images are applied.

Reflection holograms without opaque backing layer and transmission holograms both remain transparent if not illuminated. Thus they can serve as optical combiners themselves – leading to very compact displays. The illumination and rendering techniques that are described in these sections are the same for both hologram types.

Figure 2 illustrates an example of how a transmission hologram can be combined effectively with a flat-panel lenticular lens sheet display (a variation of a parallax display that utilizes refraction of a lens array to direct the light into the different viewing-zones).

Placing a transmission hologram in front of a mirror beam combiner allows to illuminate it from the front and to augment it with graphics from the back. For reflection holograms, this beam combiner is not necessary.

A thin glass plate protects the emulsion from being damaged and keeps it flat to prevent optical distortion. The lenticular lens sheet directs the light emitted from the LCD array through all layers towards the eyes of the observer. The projected light is transmitted through the first two layers, and is partially reflected back (either by the beam combiner in combination with a transmission hologram or by a reflection hologram) – reconstructing the recorded content. The remaining portion of light that is transmitted through all layers is mostly absorbed by the screen.

The following sub-sections will describe possibilities of using a digitized reference wave for reconstructing optical holograms.

2.1 Partially Reconstructing Object Waves

As described above, it is possible to reconstruct the object wave of a hologram only partially, leaving gaps where graphical elements can be inserted (cf. figure 19e, for example). Both reflection holograms (without an opaque backing layer) and transmission holograms remain transparent if not illuminated. Thus, they can serve as optical combiners—leading to very compact displays. Real-time computer graphics can be integrated into the hologram from one side, while illuminating it partially from the other side [1].

Thereby, rendering and illumination are view-dependent and have to be synchronized. If autostereoscopic displays are used to render 3D graphics registered to the hologram, both holographic and graphical content appear three-dimensional within the same space. If depth information of both is known, correct occlusion effects between hologram and graphics can be generated. Different approaches of acquiring depth information directly from a white-light hologram are explained in section 3.

Figure 3 shows a rainbow hologram of a dinosaur skull combined with graphical representations of soft tissue and bones (data provided by Lawrence Witmer of Ohio University). If the holographic plate is illuminated with a uniform light, the entire hologram is reconstructed (fig. 3-left). If the plate is illuminated only at the portions not occluded by graphical elements, the synthetic objects can be integrated by displaying them on the screen behind the plate (fig. 3-right). Technical details on display prototypes will be presented in section 4.1.

Figure 4 illustrates how the selective illumination on the holographic plate is computed to reconstruct the portion of the hologram that is not occluded by graphics.

The following outlines how rendering and illumination can be realized with conventional graphics hardware. It is assumed that depth information of the holographic content (H), as well as a scene description of the graphical content (G) are available. Both contents are geometrically aligned during an offline registered step. If optical markers are recorded in the hologram together with the actual content, cameras can be used to perform this registration automatically. In addition, the extrinsic and intrinsic parameters of the video projector (P) with respect to the holographic emulsion (E) have to be known. They are also determined during an offline calibration step. If it is mechanically possible to mount the holographic emulsion close to the graphical display (i.e., the distance between E and D is small), then E and D can be approximated to be identical.

First, an intermediate texture image (T) is created from V over E by rendering H into the graphics card's depth buffer and filling the card's frame buffer entirely with predefined light color values. In addition, G is rendered into depth and stencil buffers. The stenciled areas in the frame buffer are cleared in black and the result is copied into the memory block allocated for T.

Note that if a render-to-texture option is provided by the graphics card, the read-back operation from frame buffer into the texture memory is not necessary. The final illumination image (I) is

rendered from P by drawing E into the frame buffer and texturing E's geometry with T. The illumination image (I) is beamed onto the holographic emulsion (E) with the projector (P).

Second, a rendering image (R) is generated from V over D (off-axis) by rendering H into the depth buffer, and G into depth and frame buffers. The rendering image (R) is displayed on the graphical display (D).

This can be summarized with the following rendering algorithm:

```
create intermediate texture T from V over E (first pass):
    render H into depth buffer
    fill frame buffer with light color
    render G into depth and stencil buffer
    fill stenciled areas in frame buffer with black

render E from P textured with T and display on projector (second pass)

create rendering image R from V over D (optical inlay):
    render H into depth buffer
    render G into depth buffer and frame buffer
    display G on projector
```

Note that the projected illumination image has to be defocused (optically or digitally) to avoid displaying sharp edges or other image features on the holographic plate which the observer might focus at (which would lead to an inconsistent depth perception).

2.2 Modifying Amplitude Information

The reconstructed object wave's amplitude is proportional to the reference wave's intensity. In addition to using an incomplete reference wave for reconstructing a fraction of the hologram, intensity variations of the projected light permit local modification of the recorded object wave's amplitude.

Practically, this means that to create the illumination image (I) which is sent out by the projector, graphical shading and shadowing techniques are used to reconstruct the hologram instead of illuminating it with a uniform intensity. To do this, the real shading effects on the captured scenery caused by the real light sources used for illumination during hologram recording, as well as the physical lighting effects caused by the video projector on the holographic plate, must both be neutralized. Next, the influence of a synthetic illumination must be simulated [1].

Using conventional graphics hardware, it becomes possible not only to create consistent shading effects, but also to cast synthetic shadows correctly from all holographic and graphical elements onto all other elements.

Figure 5 shows the same rainbow hologram as in figure 3 with 3D graphical elements and synthetic shading effects. Shadows are cast correctly from the hologram onto the graphics and vice versa. A virtual point-source of light was first located at the top-left corner (L_1 in fig. 5-left), and then moved to the top-right corner (L_2 in fig. 5-right), in front of the display. Moving the virtual light source and computing new shading effects can be done in real-time. Note, that only intensity/shading variations are simulated in figure 3. A vertical variation of the object wave's wavelength that is due to diffraction effects of the rainbow hologram is still visible and cannot be corrected. This is not the case for white-light reflection holograms.

As for the algorithm explained in section 2.2 and illustrated in figure 6, multi-pass rendering can be applied to achieve these effects: For the first image (I_1), H is rendered from V over E with a white

diffuse material factor and graphical light sources that generate approximately the same shading and shadow effects on H as the real light sources that were used during the holographic recording process. This results in the intermediate texture T_1 . I_1 is generated by rendering E from P and texturing it with T_1 . It simulates the intensity of the recorded object wave. The same process is repeated to create the second image (I_2) – but this time graphical light sources are used to shade H under the new, virtual lighting situation. The ratio I_2/I_1 represents the required intensity of the reference wave at holographic plate E.

For the third image (I_3), E is rendered from P with a white diffuse material factor and a virtual point light source located at the projector's position. This intensity image represents the geometric relationship between the video projector as a physical point light source and the holographic plate:

$$F = \cos(\theta)/r^2$$

It contains form factor components, such as the square distance attenuation (r^2) and the angular correlation ($\cos(\theta)$) of the projected light onto the holographic plate and allows neutralizing the physical effects of the projector itself.

The final illumination image (I) can be computed in real time with $I = I_2/I_1/I_3$ via pixel shaders. The projection of I onto E will neutralize the physical and the recorded illumination effects as good as possible, and will create new shadings and shadows based on the virtual illumination. Note that as described previously the graphical content has to be stenciled out in I before displaying it.

During all illumination and rendering steps, hardware-accelerated shadow mapping techniques are used to simulate real and virtual shadow effects on H and on G. Finally, synthetic shadows can be cast correctly from all elements (holographic and graphical) onto all other elements.

The following rendering algorithm summarizes this approach:

```
create intensity image I1 (first pass):
  render H from V over E (white diffuse factor)...
  ...and graphical light sources that simulate real...
  ...shading on H → T1
  render E from P textured with T1

create intensity image I2 (second pass):
  render H from V over E (white diffuse factor)...
  ...and graphical light sources that simulate virtual...
  ...shading on H → T2
  render E from P textured with T2

create intensity image I3 (third pass):
  render E from P (white diffuse factor)...
  ...and graphical point light source attached to P

create and display illumination image I from P (fourth pass):
  I = I2/I1/I3 (via pixel shader)
```

The capabilities of this technique are clearly limited. It produces acceptable results if the recorded scenery has been illuminated well while making the hologram. Recorded shadows and extreme shading differences cannot be neutralized. Furthermore, recorded color, reflections and higher-order optical effects cannot be cancelled out either.

Projecting an intensity image that contains new shading and shadow effects instead of a uniform illumination allows neutralizing most of the diffuse shading that is recorded in the hologram and produced by the projector. The holographic and graphical content can then be consistently illuminated (creating matching shading and shadow effects) under a novel lighting. Since all the

discussed rendering techniques (like shadow mapping and shading) are supported by hardware-accelerated consumer graphics cards, interactive frame rates are easily achieved.

Using the concept described in this section a pallet of different display variations can be developed. With only minor changes of the presented techniques, for example, arbitrarily curved shapes (such as cylindrical shapes being used for multiplex holograms) can be supported instead of simple planar plates. Even without graphical augmentations, the projector-based illumination alone holds several potentials. In combination with optical or digital holograms it can be used to create visual effects. Certain portions of a hologram, for instance, can be made temporarily invisible while others can be highlighted. Emerging large-scale autostereoscopic displays and existing stereoscopic projection screens allow to up-scale the proposed concept, as discussed in section 5. Not only the display, but also the holograms can be composed from multiple smaller tiles to reach large dimensions and high resolutions.

3. EXTRACTING DEPTH INFORMATION FROM HOLOGRAMS

Depth information of the recorded holographic content is essential for correct rendering and interaction in combination with augmented graphical elements. The shading and occlusion effects that are presented in sections 2.1 and 2.2, as well as the force-feedback simulation that is discussed in section 4.4 would not be possible without knowing the surface geometry of the holographic content. For demonstrating the capabilities of the various techniques, the object's surface geometry has been laser-scanned before recording it as a hologram. The scanned geometric model is then registered to its holographic counterpart during a pre-process. This allows computing estimated depth values of the surfaces recorded in the hologram. However, since the original objects are usually not available for scanning after the recording process, the depth information has to be extracted directly out of the hologram.

Several approaches for extracting depth information from optical holograms have been developed. Ultra-fast holographic cameras, for instance, have been modified to allow capturing 3D objects, such as faces [20] or bodies [21]. A fast pulsed laser with short exposure time ($25ns$) is used in these cases for holographic recording that is free of motion artifacts. The depth information is then reconstructed by illuminating the hologram with a laser. Topometric information is retrieved by digitizing the real holographic image that is projected onto a diffuse plate. Moving the plate in the depth direction (away from the holographic plate) results in several 2D slices through the holographic image. These slices are finally combined to form the corresponding 3D surface.

Another approach measures the shape of a recorded surface by determining the time for light to travel from different points of the object [22]. They are based on the holographic light-in-flight technique [23].

The sections below describe the results of two other techniques for estimating holographic depth information using a flatbed scanner [31] and using a range scanner.

3.1 Depth Reconstruction Using Flatbed Scanners

Two commercial types of flatbed scanners exist today: Most scanners apply a CCD (charge-coupled device) array that captures a parallel projected image in the moving direction of the scanning slit and a perspective projected image in the other direction. A new optical technology has been

introduced by Canon –called LIDE (LED InDirect Exposure)– to reduce the size of scanners. An array of parallel rod lenses over the entire scanner width creates a parallel projection in both directions. Thus, a LIDE scanner represents a parallel perspective camera with a low focal depth.

The LIDE technology was used to scan multiple images of a hologram by placing the holographic film on top of the scanner window, leaving the lid open and illuminating it under different illumination angles for each scan (cf. figure 7). The geometric image distortion that is caused by the different illuminations [26] is captured with a parallel camera model defined by the scanner. In this case, an analytical solution exists for computing depth information if the correspondences between 2D image projections (disparities) are known [31].

Common 3D scanning techniques analyze images that are taken from cameras located on the same base-line by searching for pixel correspondences along a single direction. Due to the complex warping behavior of holograms when they are illuminated under different situations [26] the method described below requires computing 2D disparities. An algorithm that uses a hierarchical stereo matching strategy using the discrete wavelet transform (DWT) [28] is being applied for this. As mentioned above, the hologram is reconstructed from at least two different (but known) light positions. Images of the hologram are scanned with a LIDE flatbed scanner while being illuminated from these positions. If the correspondences between a minimum of two images are known it is possible to estimate depth values. More images that are recorded under additional light positions can add redundancy and consequently enhance the outcome. However, the cross-correspondence between single image pairs has still to be computed. Thus only the analytical solution for the basic case of computing depth from two parallel perspective images is described.

With the computed disparities it is aimed at estimating the depth z_o of all visible pixels. The geometric imaging behavior of holograms under different lighting conditions has been well understood [26]. Based on this model, a numerical method has been derived that estimates the image position of recorded objects for cases in which the recording reference beam does not match the reply reference beam, and a known perspective viewing situation is assumed [27]. This is illustrated in figure 8.

Since the LIDE scanner provides a parallel projection in both directions, an analytical solution can be found. For a parallel projection, the viewpoint e can be assumed to be located at infinity. Because of this the principal ray points p_i are known for both lighting positions c_1 and c_2 : $x_p = x_i$ and $y_p = y_i$. Thus, the reconstructed image points i_i of a recorded object o and the position of the viewer e are collinear. With these two constraints the equation that can be derived for the perspective case [27] reduces to:

$$0 = \frac{x_c - x_i}{R'_c} + \mu \left(\frac{x_o - x_i}{R'_o} - \frac{x_r - x_i}{R'_r} \right) \quad (1)$$

This also holds for the other dimension:

$$0 = \frac{y_c - y_i}{R'_c} + \mu \left(\frac{y_o - y_i}{R'_o} - \frac{y_r - y_i}{R'_r} \right) \quad (2)$$

Note, that $\mu = \lambda_c / \lambda_r$ where λ_c is the reconstruction wavelength and λ_r is the recording wavelength. This ratio can vary slightly from the theoretical value due to changes in humidity during reconstruction. Note also, that the radii R are measured from the origin 0 while the radii R' are measured from the corresponding principle ray points p_i . The origin and the principle ray points lie

on the holographic plane. Equations (1) and (2) are valid for all light positions. Solving these equations for x_0 and y_0 we receive:

$$x_0 = R'_{o1} \underbrace{\left(\frac{x_r - x_{i1}}{R'_{r1}} - \frac{x_{c1} - x_{i1}}{\mu R'_{c1}} \right)}_a + x_{i1} \quad \text{and} \quad x_0 = R'_{o2} \underbrace{\left(\frac{x_r - x_{i2}}{R'_{r2}} - \frac{x_{c2} - x_{i2}}{\mu R'_{c2}} \right)}_b + x_{i2} \quad (3)$$

$$y_0 = R'_{o1} \underbrace{\left(\frac{y_r - y_{i1}}{R'_{r1}} - \frac{y_{c1} - y_{i1}}{\mu R'_{c1}} \right)}_c + y_{i1} \quad \text{and} \quad y_0 = R'_{o2} \underbrace{\left(\frac{y_r - y_{i2}}{R'_{r2}} - \frac{y_{c2} - y_{i2}}{\mu R'_{c2}} \right)}_d + y_{i2} \quad (4)$$

From equation (3) follows:

$$R'_{o1} = \frac{bR'_{o2} + x_{i2} - x_{i1}}{a} \quad (5)$$

Equation (4) yields:

$$R'_{o1} = \frac{dR'_{o2} + y_{i2} - y_{i1}}{c} \quad (6)$$

With equations (5) and (6) R'_{o2} can be calculated, and with known R'_{o2} the depth for every projected object o is:

$$z_o = R'_{o2} \sqrt{1 - \frac{(x_o - x_{i2})^2}{R'_{o2}{}^2} - \frac{(y_o - y_{i2})^2}{R'_{o2}{}^2}} \quad (7)$$

Note, that correct disparities (which define the correspondences between the two images i_1 and i_2) are essential for computing the correct depth values. This still represents a main challenge.

3.2 Depth Reconstruction Using Range Scanners

Reconstructing depth information from large holograms is impossible with conventional flatbed scanners. For these hologram types, other techniques become more efficient. Range scanning is one possibility.

Common active range sensors apply a controlled illumination (structured light) together with camera feedback for estimating depth. Thus they avoid the correspondence problem that is mentioned above. However, structured light scanning cannot be used for reconstructing holographic depth information: Correspondences could be found only on the holographic plate –even if the controlled light source matches the replay light source. This leads to the depth of the holographic plate rather than to the depth of the holographic content.

But replaying the whole hologram with an unstructured projection (or an analog light source) allows using passive range sensors. Passive range sensors rely on the input from two or more calibrated perspective cameras, and on correlating the images geometrically. The main advantage over the technique described above is that –after image rectification– disparities need to be searched only in one dimension, rather than in two. Replaying the hologram with the correct illumination also avoids any geometric warping of the content. Thus, conventional two-view or multi-view geometry techniques can be used for reconstructing the depth, once the disparities have been determined. Applying range scanning to small holograms, however, is impractical due to the sensors' low precision and the holograms' limited field of view: Scanning the content close to the hologram restricts the scanning angle of the sensor. Scanning the content from an adequate distance which permits a larger angular scanning range does not allow dissolving small features that are used for

image correlation. In both cases, the holographic content can be scanned only partially. Consequently, the technique described in section 3.1 is preferred for small white light holograms.

Figure 9 illustrates the depth information reconstructed from a large (170cm x 103cm) rainbow hologram of a Tyrannosaurus rex skull (cf. figure 9a). A two-lens stereo camera system (cf. figure 9b) was used for scanning the hologram. Since the cameras have a limited field of view and the holographic content has to be reconstructed from multiple perspectives, multiple scans were captured from different horizontal angles (the rainbow hologram does not contain a vertical parallax). Each scan results in a 3D point cloud of approximately 3,500-7,000 points on different fractions of the skull's surface. The different point clouds have to merge into a common coordinate system to form the whole surface. This is achieved by determining the range sensor's position and orientation relative to the holographic plate with an infrared tracking system (cf. figure 9c). Multiple fractional point clouds can be registered into a common coordinate system by first aligning them roughly with the transformation provided by the tracking system, and then matching them using numerical closest-point iterations [34].

The center row and column of figure 9 show four registered point clouds with a total of 19,200 points. They are rotated in horizontal and vertical directions to illustrate the surface coverage.

Due to the limited resolution of the range sensor, small gaps appear between the actual surface points. To obtain continuous depth information, the points can be triangulated. This leads to a connected triangle mesh that allows estimating the missing depth information via interpolation. Triangulation of such an unstructured point cloud, however, is difficult. Due to the complex topology of the point cloud, automatic triangulation methods will most likely create wrong connectivities between points. This leads to a significant amount of manual post processing. Instead of triangulating the points into a mesh of triangle primitives, the points remain unconnected. They are rendered as point primitives with appropriate radii to fill the gaps of missing surface information (cf. figure 9d). Such a point-based rendering concept is referred to as *splatting* [33]. As it will be described in section 5, splatting provides fast and adaptable frame rates, as well as a continuous representation of a discretized surface.

4. INTERACTING WITH AUGMENTED HOLOGRAMS

Interactivity is clearly one of the success factors of modern computer graphics. CGH has a great potential to provide truly interactive holograms. However, several technological hurdles have to be taken before this will become a real competitor to computer graphics. Combining holograms and interactive computer graphics represents an intermediate solution that can be achieved today with off-the-shelf equipment. The following sections describe current experimental display prototypes and present several interaction forms in combination with different hologram types.

4.1 Display Prototypes

Figure 10 shows two desktop prototypes [31] and figure 19a illustrates a large screen prototype. They serve as proof-of-concept configurations and as testbeds for experiments. While the large screen configuration is explained in more detail in section 5, this section focuses on the desktop prototypes. The stereoscopic version (figure 10-left) consists of a conventional CRT screen with active stereo glasses, wireless infrared tracking, and a touch screen in front of the hologram for

interaction. The autostereoscopic version uses an autostereoscopic lenticular-lens sheet display with integrated head-finder for wireless user tracking and a force feedback device [9] for six degrees-of-freedom interaction.

For the autostereoscopic display prototype, a digital light projector (DLP) is applied for illuminating the hologram. Since the DLPs' time-multiplexed generation of light intensities causes synchronization conflicts with the shuttering of the active LC glasses, an LCD projector is used for the stereoscopic version instead.

A single PC with a dual-output graphics card renders the graphical content on the screen and the illumination for the holographic plate on the video projector. In both cases, the screen additionally holds further front layers (cf. figure 2) –glass protection, holographic emulsion, and optional mirror beam combiner (used for transmission holograms only).

Interaction with the graphical content is supported with a mouse, a touch-sensitive transparent screen mounted in front of the holographic plate, or a 6DOF force feedback device (see section 4.4). In addition, a camera is mounted close to the projector to detect retro-reflective markers that are attached to the holographic plate. Using structured light probes ensures a fully automatic registration of the holographic plate and calibration of the projector.

4.2 Increasing Viewing Range With Multiplex Stereograms

Digital holography uses holographic printers to expose the photometric emulsion with computer-generated or captured images. This results in conventional holograms with digital content rather than real scenery. Pre-processed 2D and 3D graphics or digital photographs and movies can be printed. This allows to holograph, for instance, completely synthetic objects, real outdoor sceneries, and objects in motion - which is difficult and sometimes impossible to achieve with optical holography. Like optical holograms, digital holograms can be multiplexed. This allows to divide the viewing space and to assign individual portions to different contents. The content for digital holograms can easily be created by non-experts, and the printing process is inexpensive. Usually a 3D graphical scene, a series of digital photographs or a short movie of a real object is sufficient for producing digital holograms. But digital holograms lack in the quality (resolution, color appearance, sharpness, etc.) of optical holograms.

Figure 11 shows a digital color white-light reflection stereogram of a car's head-light [31] (data provided by Holger Regenbrecht and Wilhelm Wilke, DaimlerChrysler AG). It was generated by taking 360 perspective photographs from different angles (in 0.5 degree steps to cover a 110° total viewing zone plus two 35° clipping areas). The perspective photographs were multiplexed into different sub-zones ($40^\circ=80$ images for the front view + $2 \times 35^\circ=140$ images for the side and rear views + $2 \times 12.5^\circ=50$ images to fill the partially visible clipping area outside the 110° total viewing zone + $2 \times 22.5^\circ=90$ images to fill the invisible clipping area outside the 110° total viewing zone). Consequently, three different partial views (front, rear, and side) can be observed by moving within the total viewing zone of 110°. After registering the holographic plane and calibrating the projector, interactive graphical elements, such as wire-frame or shaded CAD data can be integrated into the hologram. Since the head motion of the observer is tracked and the recorded viewing angles are known, the perspective of the graphical content can be updated to match the corresponding perspective recorded in the hologram. Thus, graphical and holographic content remain registered – regardless of the observer's viewing direction. This supports a non-continuous surround view of recorded and augmented scenes.

4.3 Holographic Windows

The ability to digitally control the reconstruction of a hologram allows integrating them seamlessly into common desktop-window environments. If the holographic emulsion that is mounted in front of a screen is not illuminated, it remains transparent. In this case the entire screen content is visible and an interaction with software applications on the desktop is possible in a familiar way. The holographic content (visible or not) is always located at a fixed spatial position within the screen/desktop reference frame. An application that renders the graphical content does not necessarily need to be displayed in a full screen mode (as in the examples above), but can run in a windows mode - covering an arbitrary area on the desktop behind the emulsion. If position and dimensions of the graphics window are known, the projector-based illumination can be synchronized to bind the projected light to the portion of the emulsion that is located directly on top of the underlying window.

Thereby, all the techniques that are described in section 2 (partial reconstruction and intensity variations) are constrained to the window's boundaries. The remaining portion of the desktop is not influenced by the illumination, the graphical or the holographic content. In addition, the graphical content can be rendered in such a way that it remains registered with the holographic content - even if the graphical window is moved or resized. This simple, but effective technique allows a seamless integration of holograms into common desktop environments. It allows to temporarily minimize the *holographic window* or to align it over the main focus while working with other applications. Figure 12 shows a holographic window [31] in different states on a desktop together with other applications. It displays an optical (monochrome) white-light reflection hologram of a dinosaur skull with integrated graphical 3D soft tissues. A stereoscopic screen was used in this case, because autostereoscopic displays (such as lenticular screens or barrier displays) do not yet allow an undisturbed view on a non-interlaced 2D content (such as text with a small font).

4.4 Force-Feedback Interaction

Interaction devices, such as Massie's PHANTOM [9], allow to feel computer generated 3D content by simulating force feedback. Depending on the position of the 6DOF stylus-like device (cf. figures 10-right and 13), force vectors and magnitudes are calculated dynamically based on pre-defined material parameters of the corresponding holographic or graphical content. This enables the user to virtually touch and feel the hologram and the integrated virtual models [31]. For both content types a 3D geometrical model is required to determine surface intersections with the stylus, which lead to the proper force computations. The device is installed outside the user's viewing volume and allows controlling a 3D cursor remotely. This prevents from occluding parts of the screen or casting shadows from the projected light.

While the holographic content is static, the graphical content can be deformed by the device in real time. As in some of the previous examples, a reflection hologram of a dinosaur skull has been augmented with reconstructed soft tissue. Using the force feedback device allows touching and feeling bones and muscles with different material parameters. While bones feel stiff, muscles and air sinus feel differently soft. In addition, the soft tissue can be pushed in under increasing pressure, and expand back when released. Furthermore, measurements of distances can be taken by touching arbitrary points in space with a virtual measuring tool that is controlled by the stylus.

Other groups have experimented force feedback interaction in combination with static reflection transfer holograms [10], edge-illuminated holograms [11], and dynamic electroholograms [12,13].

Note, that in contrast to CGHs, optical holograms are static. A modification of the holographic content is not possible in this case. This is also true for our approach. Only the graphical content can be dynamically modified. However, force feedback can be simulated for both - the holographic and the graphical part.

4.5 Touch Interaction

A transparent and touch-sensitive surface can be used as front layer to support touch and pointing interactions. The prototype illustrated in figure 14 applies a resistive analog touch screen with an invisible spacer, a touch resolution of 2048x2048 on a surface of 30x40cm, an 80% nominal light transmission, 10ms responds time and a maximum error of 3mm. Touch events are activated through pressure – by finger, fingernail, gloved hand or stylus. The resulting 2D position of the pointer on the registered panel in combination with the head-position of the observer (known from head-tracking) leads to a 3D ray that can be used by ray-casting techniques to select holographic or graphical objects that are intersected by the ray.

In the example shown in figure 14, touch interaction is used for operating the recorded keypad of a car navigation system [31] (data provided by Holger Regenbrecht and Wilhelm Wilke, DaimlerChrysler AG). A high-quality full color Denisjuk hologram replays the console while monoscopic or autostereoscopic graphics is integrated into the console's original LCD panel. This allows simulating novel 2D/3D graphics interface designs, as well as new interaction and presentation schemes for navigation systems under realistic evaluation conditions before building physical prototypes. Touching the surface above a recorded button triggers the specific function of the system and the augmented graphics panel is updated with the corresponding content.

4.6 Augmenting Volumetric Multiplexed Holograms

Volumetric multiplexed holograms [24] are digital multiple exposure transmission holograms that contain static CT, MRI or other volumetric datasets. They encode slices from a medical scan on a holographic film. The slices can be reconstructed simultaneously and appear as semi-transparent in space – resulting in a three-dimensional volumetric image. In contrast to many other 3D display techniques that are applied for viewing medical data, volumetric multiplexed holograms share the properties of other hologram types and support all depth queues. This is also the case for electroholographic displays. Some experiments have been made recently to use such devices for presenting time-series volumetric data [25].

Although the recorded content is static, volumetric multiplexed holograms can be augmented with interactive stereoscopic graphics.

The *Voxbox* display [24] is an analog light-box-like display that consists of a small tungsten halogen lamp, a front-surface mirror, and a sandwich of a Fresnel lens, a diffraction grating with dispersion compensation and a light directing film. It is used to replay volumetric multiplexed holograms. The mirror of the *Voxbox* display virtually places the lamp at the focal point of the lens. The collimated light behind the lens is diffracted at an angle to reconstruct the hologram, and dispersed to cancel its strong dispersion effects. A louver film between the grating and the hologram blocks the zero-order light while letting the grating's dispersed spectrum pass through the hologram.

To integrate stereoscopic computer graphics into the volumetric hologram [31], the halogen lamp and the mirror are replaced by two LCD projectors and mirror beam-combiners (cf. figure 15-top). The projected images are used to illuminate the hologram and to display colored stereo pairs at the

same time. To ensure that a focused image is projected onto the holographic plane, the original Fresnel lens is replaced by a new lens with a focal distance of $1m$. A 50/50 mirror beam combiner allows locating both projection centers at the lens' focal point. For separating the stereo images, LC shutters are attached in front of each projector's lens. These shutters are triggered in sync with the LC shutters of the observer's glasses by an external pulse generator at $100Hz$ or more. Air cooling prevents the LC shutters from being overheated. A normal (horizontal or vertical) alignment of the projectors would cause diffraction artifacts in form of visible Moiré patterns. This is because the raster of the projected pixels are in line with the orientation of the diffraction grating and the louvers of the light directing film. To minimize these artifacts, both projectors are tilted to a 45° angle around the projection axis. Note that in this case the LC shutters on the observer's glasses have to be rotated by the same angle to prevent light-loss caused by polarization effects. A wireless infrared tracking device is used to support head-tracking of the observer which is required for perspective correct rendering of the graphics for different head positions.

One projector displays the left stereo image while the other one displays the right stereo image. If the background of both images is white (or another gray scale), the holographic content is completely reconstructed. At those places where graphical elements are projected onto another color, the holographic content is blended with the graphical content. Thus, the graphical content appears also semi-transparent. A correct occlusion of holographic parts by graphical objects can only be achieved if the graphics is rendered in black (e.g., on a white background). This does not reconstruct the hologram in these areas. These techniques can be used to integrate interactive graphical augmentations into the hologram, or to color code different parts in a volumetric model, as illustrated in figure 15-bottom. This opens a variety of new interaction possibilities with volumetric multiplexed holograms, which still have to be explored.

The new generation of fast DLP projectors makes the application of two optically merged projector units, as well as the external shutter system unnecessary. They provide $120Hz$ refresh rate and consequently support active stereoscopic visualizations with a single device.

5. AUGMENTING LARGE-SCALE HOLOGRAMS

A possibility for reconstruction depth from a sizable hologram was discussed in section 3.2. Large scale optical holograms, however, also require large scale display technology for combining them with interactive graphical elements. Conventional desktop displays, such as desktop-size CRTs or LCDs are not sufficient in this case. Projection technology allows generating images that are larger than the display device itself. Furthermore, the display devices can be located at a different position than the image. Consequently, projectors can be used for reconstructing the holographic content and for displaying the graphical content. In contrast to the approach described in section 4.6 where one projector (or two coaxially aligned projectors) is used to integrate the graphical elements and to replay the holographic content, two different projection channels are required for off-axis recorded holograms: one for illumination and one (or two) for displaying the graphics. In the following, these two projectors are called *illumination projector* and *display projector*.

5.1 Using The Grating As Diffuser

The diffraction gratings of optical holograms (although being transparent if not illuminated from the reconstruction angle) diffuse a fraction of the incoming light. Thus graphical images can be projected onto them from a non-reconstruction angle which leads to an observable image. The brightness of the image depends on light-throughput of the display projectors. Simultaneously, the illumination projector generates a reference wave that replays the hologram with respect to the displayed graphical content (as explained in section 2).

The images of both projectors must be geometrically aligned on the holographic plane. This is achieved with conventional multi-projector registration techniques.

Figure 16 shows an experiment with a two-dimensional content projected onto the large rainbow hologram of a Tyrannosaurus rex skull that was used for depth reconstruction in section 3.2. A finite element simulation of cranial mechanics and feeding in Tyrannosaurus rex (data provided by Emily J. Rayfield, The Natural History Museum London) has been off-axis projected onto the grating using two 1100 ANSI lumen LCD projectors.

A single consistent image has been created from both projector contributions via structured light projection and camera feedback. The geometry of both input images was warped in real-time on a per-pixel basis. The holographic content has been reconstructed in this case with an intensity controlled analog 50W halogen light bulb, rather than with an illumination projector. The content of the FEM simulation has been registered with the holographic content via a manual mesh deform during a calibration step. Note, that due to the analog reconstruction light, both – the graphical and the holographic content – appear simultaneously (semi-transparent). This allows comparing the color coded stress patterns with the underlying skull geometry. Note that the FEM data was two-dimensional and appeared on the holographic plane, while the holographic content was three-dimensional. Consequently a correct registration was provided only for a single viewpoint.

5.2 Using Shuttered Projection Screens

Projecting images directly onto the holographic grating has one main disadvantage: Most of the incoming light is transmitted and only a small fraction is being diffused. This is inefficient and leads to relatively dim images.

More efficient projection screens can be found for augmenting large-scale optical holograms. These screens, however, must not be opaque, but must transmit and diffuse light to replay the hologram and to display the graphics.

Examples for passive projection screens are semi-transparent holographic projection screens that diffuse the light in a narrow angle to achieve an enhanced brightness for restricted viewing angles, or transparent film screens that diffuse the light in a wide angle to support a more flexible viewing and a higher degree of transparency. Other examples are actively shuttered projection screens with a phase dispersed liquid crystal layer that can be switched to a diffuse and to a transparent state electronically.

Figure 17 compares a holographic projection screen (HOPS) with a shuttered projection screen (SPS). While the HOPS is passive and provides the same transmission / diffusion characteristics at all times, the SPS is active and can be switched electronically to a complete diffuse and to a complete transparent mode. When shuttering the SPS with 50Hz it provides approximately the same see-through quality as the HOPS. In the diffuse mode, however, the SPS provides a more uniform diffusion of the projected image than the HOPS (which –at a zero-degree projection– shows the hotspot of the projector lens at the center of the image).

Figure 18 illustrates a configuration that applies a large SPS to integrate graphics into the 170cm x 103cm rainbow hologram presented in figure 9. The SPS (S) is mounted behind the holographic emulsion (E). While an illumination projector (I) reconstructs the hologram as explained in section 2, the display projector(s) (D) generates the stereoscopic images of the augmented graphical content on S. Both projectors are aligned off-axis: I projects from the reconstruction angle, and D is aligned in such a way that intervisibility with the projector lens is avoided. The clock diagram in figure 18 shows the clock cycle and synchronization between S, I and D. Note that I can optionally be shuttered with an external liquid crystal shutter to allow a reconstruction of the hologram only when S is in the transparent mode. The left (L) and right (R) stereo images of the graphical scene are displayed with the twice the frequency (i.e., 100Hz in this case) of S's shutter frequency (i.e., 50Hz in this case, due to capacitive limitations of the SPS).

Figure 19 demonstrates the capabilities of such an approach. Figure 19a explains the setup: An observer who is wearing LCD shutter glasses is head-tracked via an infrared tracking system. The graphical content is rendered from the perspective of the observer and is then projected from the off-axis aligned display projector(s). Infrared emitters synchronize the shutter glasses with the time-modulated stereo pairs at approximately 100Hz. The SPS is shuttered at 50Hz, as illustrated in figure 18. The off axis aligned illumination projector replays the holographic content with respect to the graphical content as outlined in section 2.

To benefit from a larger light output, the illumination projector is not shuttered in this configuration. Thus it projects light in the transparent as well as in the diffuse state of the SPS. Due to a small gap between the SPS and the holographic plate and due to the fact that the light is being scattered in all directions in the diffuse mode, the holographic content appears achromatic and slightly blurred (cf. figure 19b). This can be reduced by minimizing the gap between hologram and diffuser. Figure 19c shows the reconstructed and splatted depth information that have been registered to the holographic content. This information is normally not visualized, but only being used for creating correct occlusion effects, as explained in section 2. The splat size and rendered resolution depends on the distance of the observer to the holographic content. If further away, a lower resolution with larger splats is chosen to increase rendering performance. If closer to the hologram, the splat size decreases while the resolution increases, to provide a higher accuracy. This technique is referred to as dynamic multi-resolution splatting [32].

Figures 19d-f finally illustrate the results: Without controlled reconstruction of the holographic content, the integrated graphical content appears semi-transparent (cf. figure 19d). Not reconstructing the holographic content in areas where graphical elements occlude holographic elements (cf. figure 19e) leads to consistent occlusion effects (cf. figure 19f). Note that the graphical content is also partially occluded by the reconstructed depth information registered to the holographic content.

Interaction with augmented large-scale holograms can be supported by existing interaction techniques known from large-screen projection displays used for virtual reality applications, such as laser-pointer interaction, or multiple-degrees-of-freedom techniques using specialized interaction devices.

6. CONCLUSION

Computer-generated holography will play an important role for future display technology. It has a high potential to provide a platform for a realistic and interactive visualization in many areas. However, several technological problems have yet to be solved before CGH will be a useful alternative to three-dimensional computer graphics. Holograms support all depth queues. An important property which most other stereoscopic and autostereoscopic displays do not provide. However, analog holograms are static and lack in interactivity.

Several rendering, illumination, interaction and reconstruction methods for combining optical and digital holograms with interactive computer graphics have been described in this chapter. They are the results from experiments carried out during a two-year research project. The discussed prototypes and setups served as proof-of-concept platforms, and do not represent professional or commercial displays.

It is clear that while the holographic content can offer all advantages of holograms (i.e. extremely high visual quality and realism, support for all depth queues at no computational cost, space efficiency, etc.), the integrated graphical part can be interactive. As illustrated, a variety of common hologram types, existing displaying methods, and potential application domains can be addressed with this concept. Computational intensive information, such as volumetric datasets or photorealistic scenes, for instance, can be represented with a hologram while interactive elements can be added with computer graphics. All of this is possible with off-the-shelf technology that is available today. This may lead to new tools for science, industry and education.

Archaeologists, for example, already use holograms to archive and investigate ancient artifacts. Scientists can use hologram copies to perform their research without having access to the original artifacts or settling for inaccurate replicas. They can combine these holograms with interactive computer graphics to integrate real-time simulation data or perform experiments that require direct user interaction, such as packing reconstructed soft tissue into a fossilized dinosaur skull hologram. In addition, specialized interaction devices can simulate haptic feedback of holographic and graphical content while scientists are performing these interactive tasks. An entire collection of artifacts will fit into a single album of holographic recordings, while a light-box-like display such as that used for viewing x-rays can be used for visualization and interaction. The same applies to the biomedical domain that already uses digital volumetric holograms produced from CT or MRI data of inner organs.

In the automotive industry, for instance, complex computer models of cars and components often lack realism or interactivity. Instead of attempting to achieve high visual quality and interactive frame rates for the entire model, designers could decompose the model into sets of interactive and static elements. The system could record physical counterparts of static elements in a hologram with maximum realism, and release computational resources to render the interactive elements with a higher quality and increased frame rate. Multiplexing the holographic content also lets users observe and interact with the entire model from multiple perspectives. Beside display holograms, holographic interferograms used for non-destructive measurement and testing are yet another example of industrial applications. Analogue interferograms that indicate motion, vibration, or deformations of objects can be combined with digital simulation data. Augmenting holograms in museums with animated multimedia content lets exhibitors communicate information about the artifact with more excitement and effectiveness than text labels offer. Such displays can also

respond to user interaction. Because wall-mounted variations require little space, museums can display a larger number of artifacts.

Figure 20 shows two illustrations of envisioned future applications: A wall-mounted display in a museum environment, with a ceiling-mounted video projector replacing conventional spotlights, and a desktop display that can be used in a light-box fashion. A special input device allowing interaction, including haptic feedback of holographic and graphical content.

The *HoloGraphics* project focused on developing basic techniques and on a proof of concept. These techniques and concepts, however, have now to pass the prototype stage. They must be evaluated by potential end users and have then to be improved.

ACKNOWLEDGEMENTS

I thank the *HoloGraphics* team at the Bauhaus-University Weimar whose work is presented in this chapter: Thomas Zeidler, Anselm Grundhöfer, Ferry Häntsch, Alexander Kleppe, Daniel Kurz, Erich Bruns, Franz Coriand, Uwe Hahne, Mathias Möhring, Sebastian Knödel, Gordon Wetzstein, and Tobias Langlotz.

Furthermore, I would like to acknowledge Yves Gentet of the Yves GENTET - Art and Science holographic studio, Stephen Hart of Voxel Inc., Kaveh Bazargan of Focal Image Ltd, Tim Frieb of Holowood Holographiezentrum Bamberg e.K., Wilhelm Wilke of DaimlerChrysler AG, Holger Regenbrecht of Otago University/ DaimlerChrysler AG, Emily J. Rayfield of the Natural History Museum London, Steven Gatesy of Brown University, and Lawrence Witmer of Ohio University for providing data, their technical support and professional feedback.

This project was supported by the Deutsche Forschungsgemeinschaft (DFG) under contract number BI 835/1-1.

REFERENCES

1. O. Bimber, Combining Optical Holograms with Interactive Computer Graphics, IEEE Computer, pp. 85-91, January 2004.
2. J.S. Kollin, S.A. Benton, and M.L. Jepsen, Real-Time Display of 3-D Computed Holograms by Scanning the Image of an Acousto-Optic Modulator, Proceedings of SPIE, vol. 1136, Holographic Optics II: Principles and Applications, Springer, pp. 178-185, 1989.
3. M. Lucente, Interactive Three-Dimensional Holographic Displays: Seeing the Future in Depth, ACM Computer Graphics, Special Issue on Current, New, and Emerging Display Systems, ACM Press, pp. 63-67, 1997.
4. M. Lucente and A. Tinsley, Rendering Interactive Images, Proceedings of ACM Siggraph'95, ACM Press, pp. 387-394, 1995.
5. M. Lucente, Interactive Computation of Holograms Using a Look-Up Table, Journal of Electronic Imaging, vol. 2, no. 1, pp. 28-34, 1993.
6. C. Petz and M. Magnor, Fast Hologram Synthesis for 3D Geometry Models Using Graphics Hardware, Proceedings of SPIE'03, Practical Holography XVII and Holographic Materials IX, vol. 5005, Springer, pp. 266-275, 2003.

7. F. Dreesen and G. von Bally, Color Holography in a Single Layer for Documentation and Analysis of Cultural Heritage, In Proceedings of Optics within Life Sciences (OWLS IV), Springer, pp. 79-82, 1997.
8. F. Dreesen, H. Deleré, and G. von Bally, High-Resolution Color Holography for Archaeological and Medical Applications, In Proceedings of Optics within Life Sciences (OWLS V), Springer, pp. 349-352, 2000.
9. T. H. Massie, and J. K. Salisbury, The PHANTOM Haptic Interface: A Device for Probing Virtual Objects Proceedings of the ASME Dynamic Systems and Control Division, vol. 55, no. 1, pp. 295-301, 1994.
10. M.R.E. Jones, The Haptic Hologram, Proceedings of SPIE, Fifth International Symposium on Display Holography, vol. 2333, pp. 444-447, 1994.
11. W. Plesniak and M. Klug, Tangible Holography: Adding Synthetic Touch to 3D Display, Proceedings of the IS&T/SPIE Symposium on Electric Imaging, Practical Holography XI, pp. 53-63, 1999.
12. W. Plesniak and R. Pappu, Coincident Display Using Haptic and Holographic Video, Proceedings of ACM SIGCHI conference on Human factors in computing systems, pp. 304-311, 1998.
13. W. Plesniak and R. Pappu, Spatial Interaction with Haptic Holograms, Proceedings of the IEEE International Conference on Multimedia Computing and Systems, vol. 1, pp. 413-426, 1999.
14. Y. Gentet and P. Gentet, Ultimate emulsion and its applications: a laboratory-made silver halide emulsion of optimized quality for monochromatic pulsed and full-color holography, Proceedings of SPIE'00, Holography 2000, vol. 4149, pp. 56-62, 2000.
15. D. Vila, Folding Time into Space – Novel Approaches to Integral Holography, Proceedings of SPIE'93, Practical Holography VII: Imaging and Materials, vol. 1914, Springer, pp. 230-235, 1993.
16. D. Vila, Holo-Dynamics – Linking Holography to Interactive Media, Proceedings of SPIE'93, Practical Holography VIII, vol. 2176, Springer, pp. 166-171, 1994.
17. M. Okamoto, H. Ueda, I. Nakamura, E. Shimizu, and T. Kubota, Multiple Illuminations Method for Rainbow Holograms using an LCD Projector, Proceedings of SPIE'97, Practical Holography XI, vol. 3011, Springer, pp. 70-75, 1997.
18. K. Yamasakia, M. Okamotoa, I. Nakamura, and E. Shimizu, Fluctuation Hologram with Multiple Images, Proceedings of SPIE'98, Practical Holography XII, vol. 3293, Springer, pp. 139-144, 1998.
19. J.R. Andrews and W.H. Haas, Compact Illuminators for Transmission Holograms, Proceedings of SPIE'89, Practical Holography III, vol. 1051, Springer, pp. 156-159, 1989.
20. J. Bongartz, D. Giel, P. Hering, Fast 3D topometry in medicine using pulsed holography, Proceedings of SPIE'02, Practical Holography XVI and Holographic Materials VIII, vol. 4659, 2002.
21. S. Frey, J. Bongartz, D. Giel, A. Thelen, and P. Hering, Ultrafast holographic technique for 3D in situ documentation of cultural heritage, Proceedings of SPIE'03, Optical Metrology for Arts and Multimedia, vol. 5146, pp. 194-201, 2003.
22. T. Carlsson, J. Gustafsson, and B. Nilsson, Development of a 3D camera, Proceedings of SPIE'99, Practical Holography XIII, vol. 3637, pp. 218-224, 1999.
23. N. Abramson, Light-in-flight recording: high-speed holographic motion pictures of ultrafast phenomena, Applied Optics, vol. 22, no. 2, pp. 215-231, 1983.

24. S.J. Hart and M.N. Dalton, Display holography for medical tomography, Proceedings of SPIE'90, Practical Holography IV, vol. 1212, pp. 116-135, 1990.
25. W. Plesniak, M. Halle, S.D. Pieper, W. Wells III, M. Jakab, D.S. Meier, S.A. Benton, C.R.G. Guttman, and R. Kikinis, Holographic Video Display of Time-Series Volumetric Medical Data, Proceedings of IEEE Visualization, pp. 78-85, 2003.
26. E.B. Champagne, Nonparaxial Imaging, Magnification, and Aberration Properties in Holography, Journal of the Optical Society of America, vol. 57, no. 1, pp. 51-54, 1967.
27. K. Bazargan, Techniques in Display Holography, Ph.D. Dissertation, Physics Dept, Imperial College, London University, p. 16, 1986.
28. H. Liu and P. Bhattacharya, Uncalibrated stereo matching using discrete wavelet transform, Proceedings of 15th International Conference on Pattern Recognition, vol.1, pp.114-118, 2000.
29. C. W. Slinger, C. D. Cameron, S. J. Coomber, R. J. Miller, D. A. Payne, A. P. Smith, M. A. G. Smith, and M. Stanley, Recent developments in computer generated holography: towards a practical electroholography system for interactive 3D visualization, Proceedings of SPIE'04, Practical Holography XVIII, vol. 5290 ,pp. 27-41, 2004.
30. C. W. Slinger, C. D. Cameron, and M. Stanley, Computer-generated holography as a generic display technology, IEEE Computer, vol 38, no. 8, pp. 46-53, 2005.
31. O. Bimber, T. Zeidler, A. Grundhöfer, G. Wetzstein, M. Möhring, S. Knödel, and U. Hahne, Interacting with Augmented Holograms, Proceedings of SPIE, Practical Holography XIX: Materials and Applications, Springer, January 2005.
32. S. Rusinkiewicz and M. Levoy, QSplat: A Multiresolution Point Rendering System for Large Meshes," Proceedings of ACM SIGGRAPH, pp. 343-352, 2000.
33. J. P. Grossman and W. Dally, Point Sample Rendering, Proceedings of Workshop on Rendering Techniques, pp. 181–192, Springer, 1998.
34. P.J. Besl, N. D. McKay, A Method for Registration of 3-D shapes, Proceedings of IEEE Transactions on Pattern Analysis and Machine Intelligence (PAMI), vol. 14 no. 2, pp. 239-256, 1992.

FIGURES

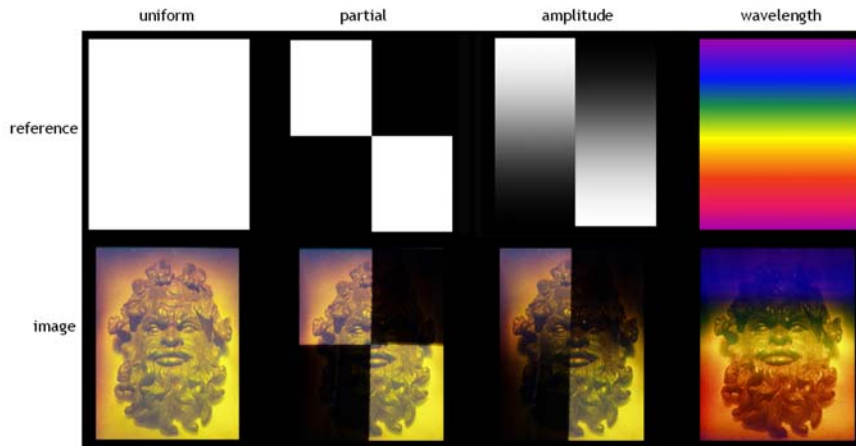


Figure 1: The projected reference waves (top row) and the resulting holographic images (bottom row). *(Image reprinted from [31] © SPIE).*

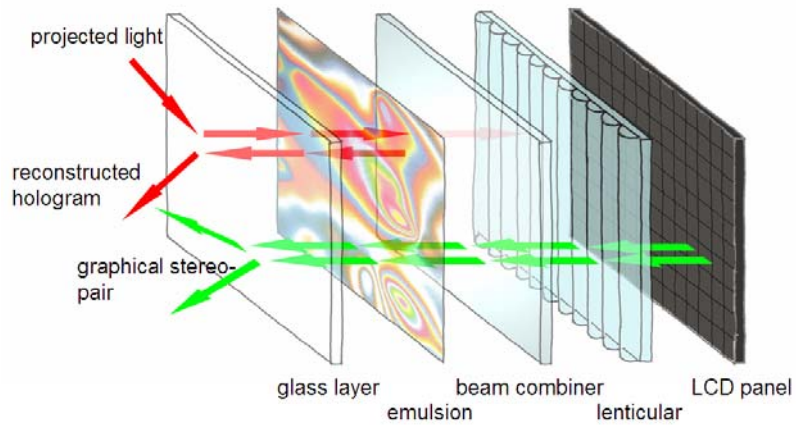


Figure 2: Explosion model of the optical layers' stacked structure. The example shows a transmission hologram in combination with autostereoscopic lenticular screen. *(Image reprinted from [1] © IEEE).*

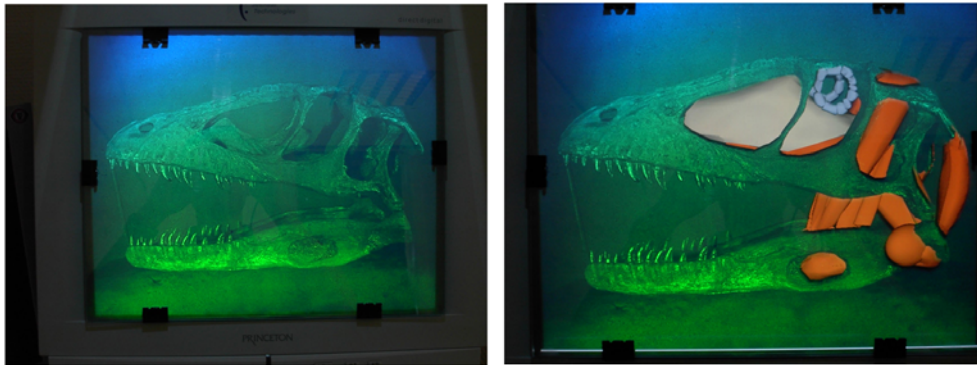


Figure 3: Rainbow hologram of a dinosaur skull combined with graphical representations of soft tissue and bones. (Image reprinted from [1] © IEEE).

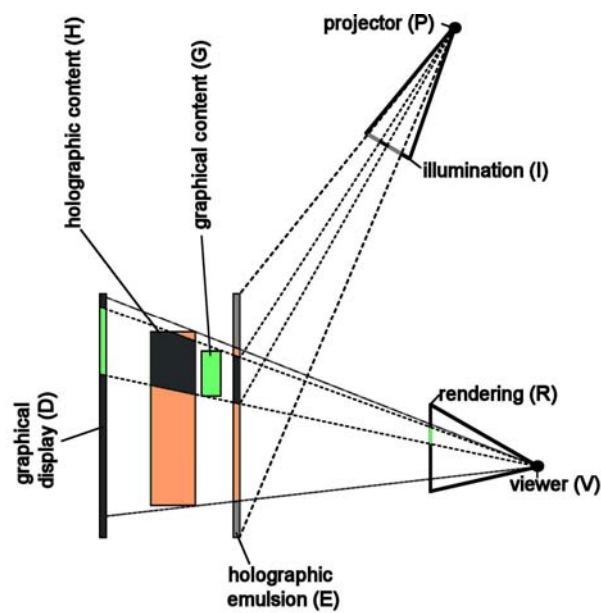


Figure 4: A conceptual sketch of the display constellation. The colored areas on the graphical display and on the holographic emulsion illustrate which portion of the visible image is hologram (red) and which is graphics (green). (Image reprinted from [1] © IEEE).



Figure 5: A rainbow hologram with 3D graphical elements and synthetic shading and shadow effects. (Image reprinted from [1] © IEEE).

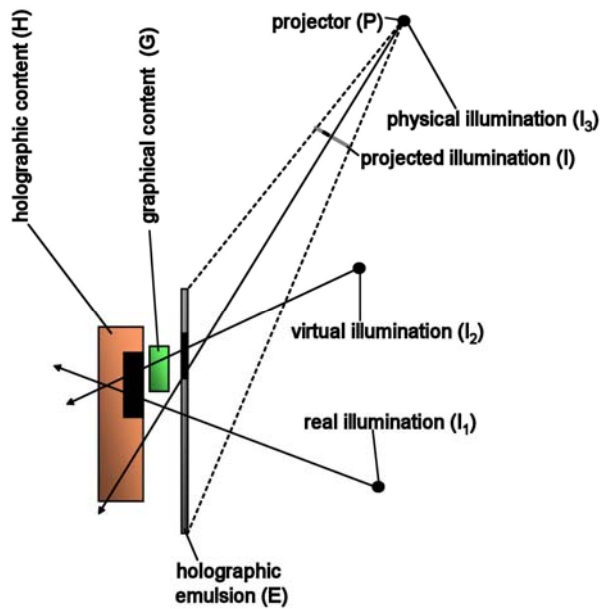


Figure 6: Light-interaction between hologram and graphics: To simulate virtual shading and shadow effects on the holographic content, the recorded and the physical illumination effects have to be neutralized. (Image reprinted from [1] © IEEE).

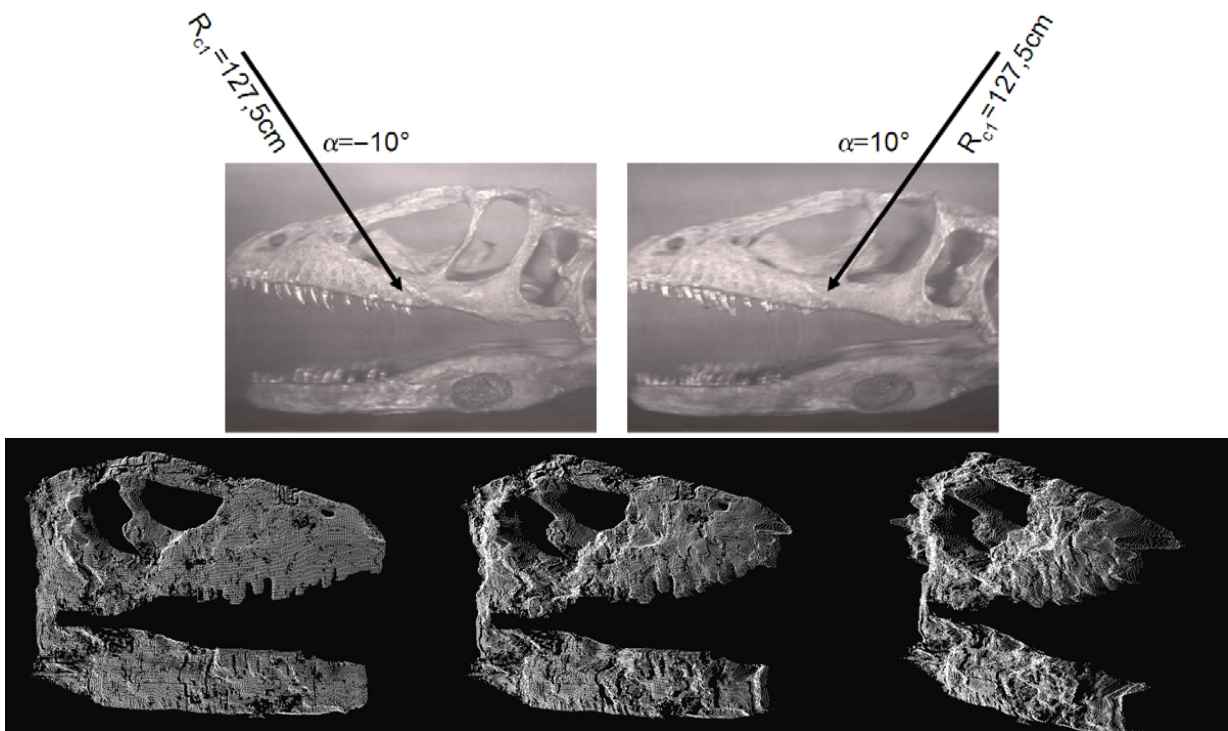


Figure 7: Two LIDE scans of a rainbow hologram with different reference wave angles (top), and point-cloud of reconstructed depth map (bottom). (Image reprinted from [31] © SPIE).

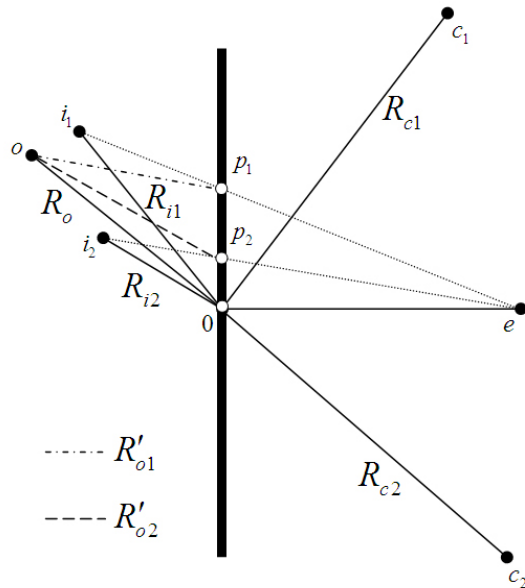


Figure 8: Flatland diagram of reconstruction geometry. (Image reprinted from [31] © SPIE).

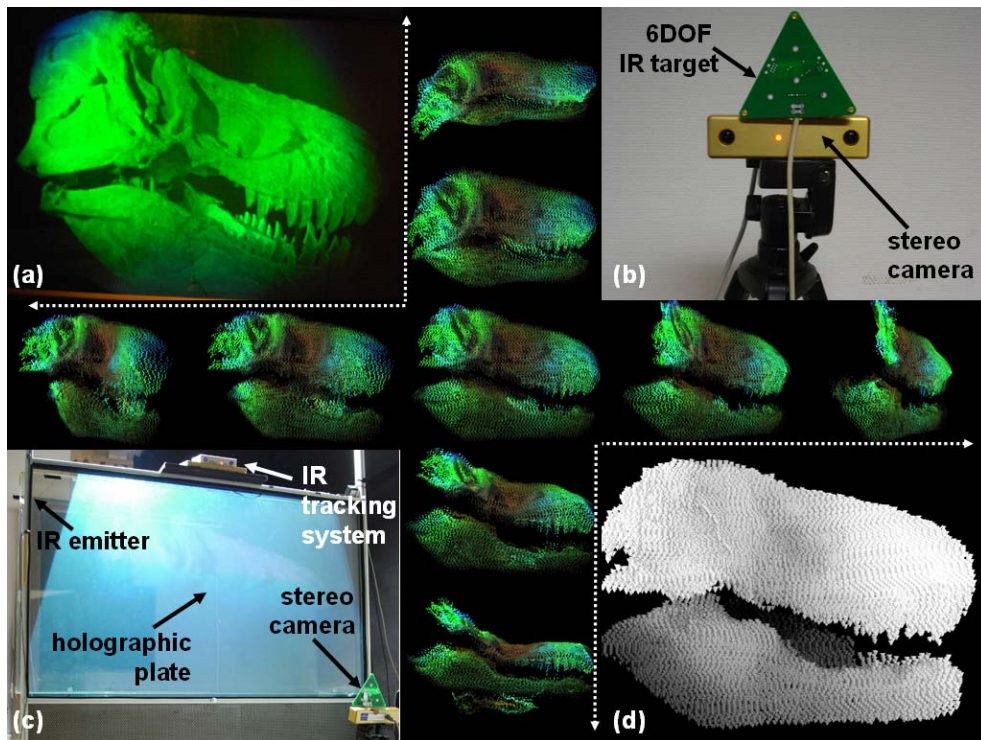


Figure 9: Reconstructing and interpolating depth from large-scale holograms via range-scanning, point matching and splatting.

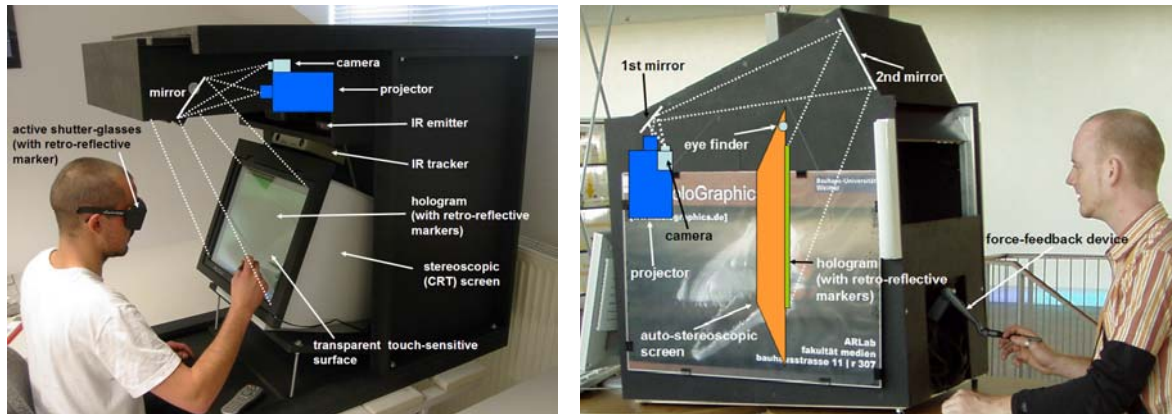


Figure 10: Stereoscopic (left) and autostereoscopic (right) display prototypes. (Image reprinted from [31] © SPIE).

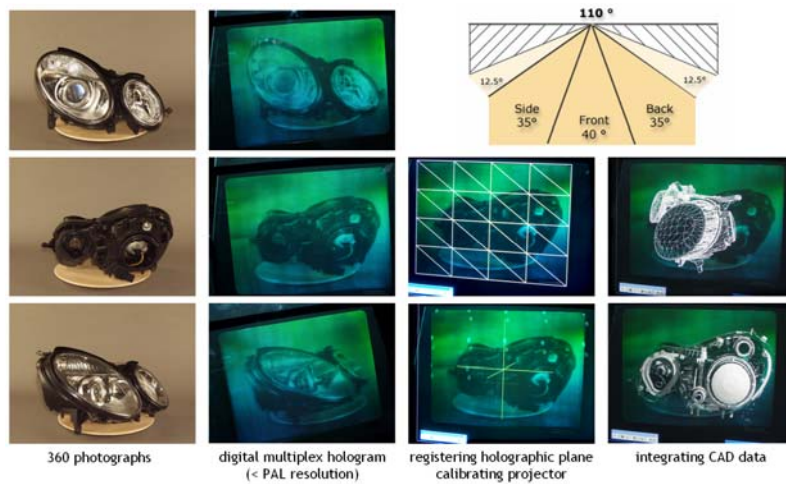


Figure 11: A multiplexed digital reflection stereogram of a car headlight with integrated CAD data. (Image reprinted from [31] © SPIE).

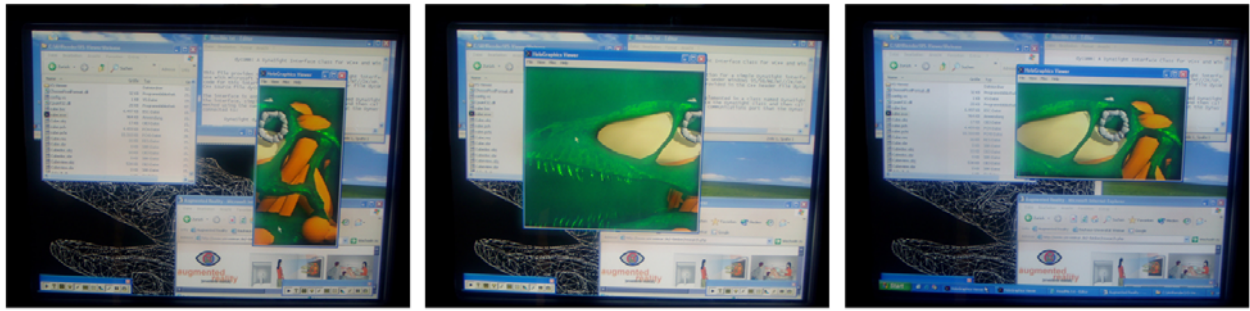


Figure 12: A holographic window in different states on a desktop together with other applications. The hologram is a white-light reflection hologram. (Image reprinted from [31] © SPIE).

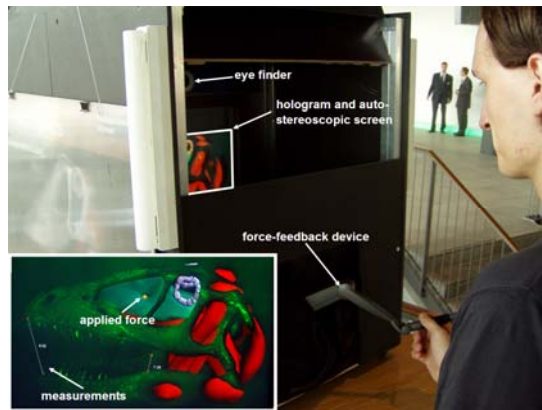


Figure 13: Force-feedback interaction with a reflection hologram of a dinosaur skull and augmented graphical soft-tissue. (Image reprinted from [31] © SPIE).

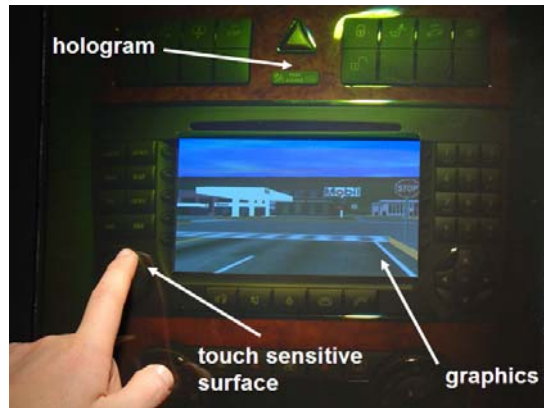


Figure 14: A full color hologram of a car navigation console. Graphics is integrated into the console's display to simulate the design of novel graphics interfaces before building prototypes. (Image reprinted from [31] © SPIE).

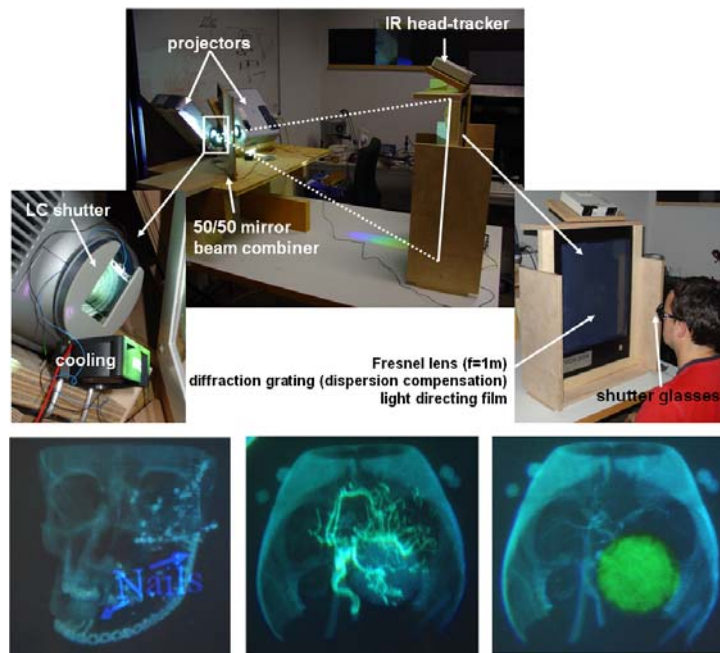


Figure 15: Prototype setup of modified *Voxbox* display (top), and sample results of holographic CT and MRI recordings with integrated stereoscopic graphics (bottom). (Image reprinted from [31] © SPIE).

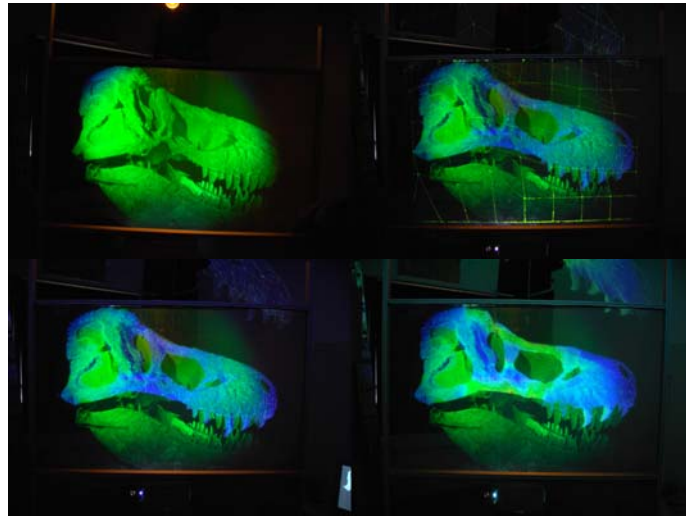


Figure 16: A large rainbow hologram of a t.rex skull with an integrated 2D FEM simulation of cranial mechanics and feeding. The graphics is projected directly onto the holographic grating.

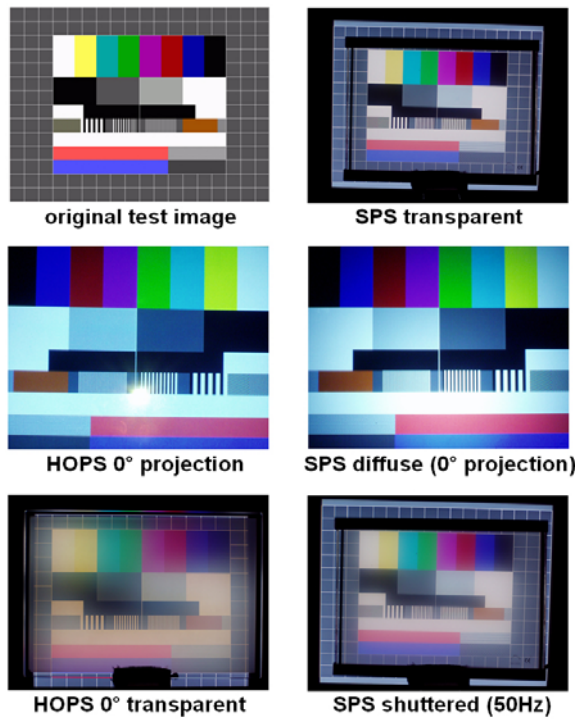


Figure 17: Comparison between passive holographic projection screen (HOPS) and active shuttered projection screen (SPS).

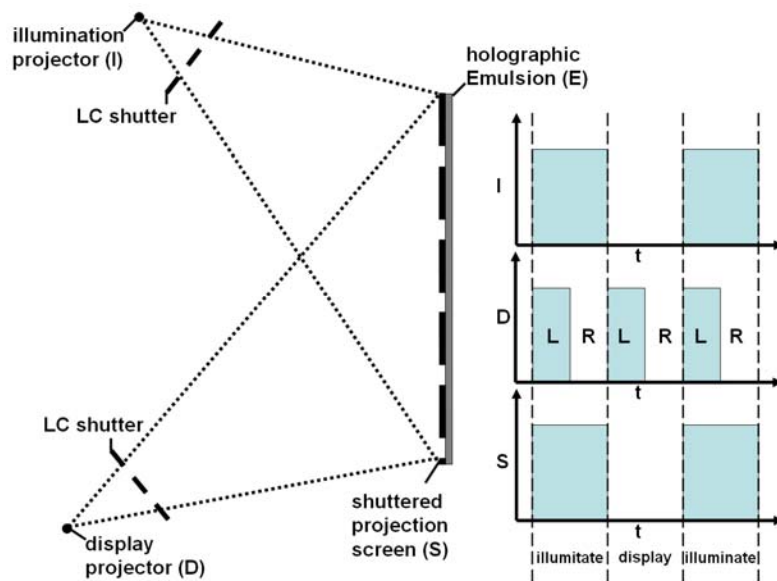


Figure 18: Using a shuttered projection screen for augmenting graphics into large-sale holograms.

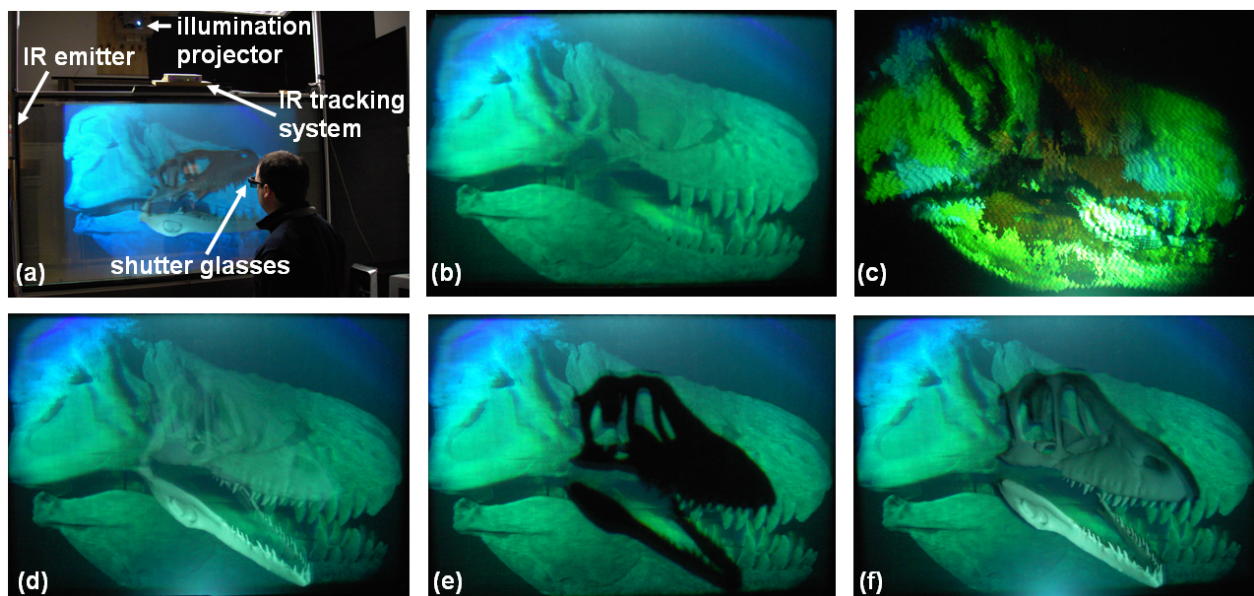


Figure 19: Example for augmenting large-scale holograms: Reconstructed depth information is registered to the holographic content while hologram is digitally replayed to produce consistent occlusion effects.

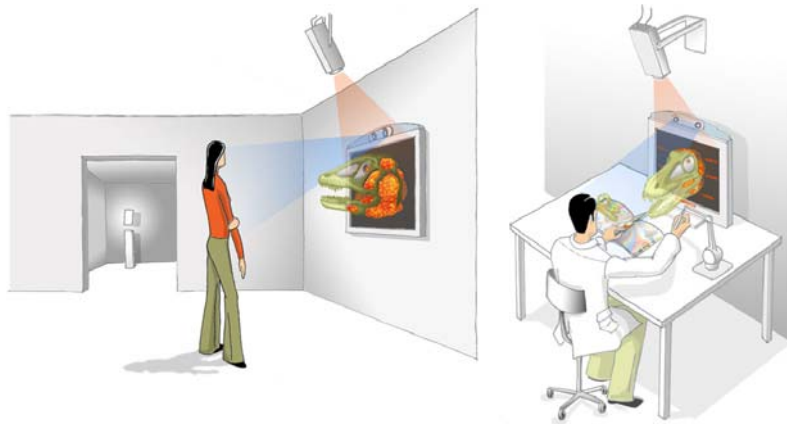


Figure 20: Illustrations of envisioned future applications: Museum displays and scientific visualization and simulation. (*Image reprinted from [1] © IEEE*).